# Stability of Fracturing Process in RC Beams

By Alberto Carpinteri[1]

**Abstract:** A reinforced concrete beam section with a through-thickness edge crack in the stretched part is considered. The eccentric axial force transmitted by the reinforcement to the concrete beam element, is estimated by means of a rotation congruence condition able to provide this statically undetermined reaction. In the field of linear elastic fracture mechanics, such a force increases linearly by increasing the external bending moment, until the limit force of yielding or slippage is reached. From this point on a perfectly plastic behavior of the reinforcement is considered. Once the bending moment of steel plastic flow is exceeded, the cracked beam segment presents a linear-hardening behavior, until the concrete fracture occurs. It is shown how the stability of the process of concrete fracture and steel plastic flow depends on the mechanical and geometrical (scale included) properties of the beam cross section.

## Introduction

In the limit analysis of a reinforced concrete beam cross section, the stretched part of concrete is conventionally assumed not to be traction bearing, while a perfectly plastic behavior of the compressed part is hypothesized (10). Such analysis does not take into consideration the cracks which usually develop in concrete and generally cause a more complex crisis phenomenon: the collapse of the concrete-steel system. In fact the limit analysis approach does not consider at all the stiffness variation and the stress concentration due to the presence of cracks. On the other hand, these two effects can be studied through fracture mechanics concepts.

Traditionally, the problems relating to cracked masonry or concrete constructions are studied on the basis of empirical parameters, such as the crack width, i.e., the distance between the crack free surfaces (1). Such parameters cannot be considered as absolute indications of the crack stability condition, but only as alarm signals of incipient collapses. In fact, the crack width will not be constant, but will generally increase, moving away from the crack tip. It will, however, depend on the sizes of the cracked structure. In the present treatment, scale effects will be emphasized in the collapse phenomena of reinforced concrete beams, as has been already done for plain concrete structures (2–5). Five types of potential collapses will be considered: (1) Crack propagation in concrete; (2) tensile strength collapse in concrete; (3) crushing collapse in concrete; (4) yielding of steel; and (5) slippage of steel.

The final collapse is generally the definitive and irreversible consequence of the five aforementioned collapses. Such collapses will occur in a well-defined sequence, according to the mechanical and geometrical (scale included) properties of the beam cross section.

[1]Research Asst., Istituto di Scienza delle Costruzioni, Univ. of Bologna, 2 Viale Risorgimento, 40136 Bologna, Italy.

Note.—Discussion open until August 1, 1984. To extend the closing date one month, a written request must be filed with the ASCE Manager of Technical and Professional Publications. The manuscript for this paper was submitted for review and possible publication on August 19, 1982. This paper is part of the *Journal of Structural Engineering*, Vol. 110, No. 3, March, 1984. ©ASCE, ISSN 0733-9445/84/0003-0544/$01.00. Paper No. 18668.

Then, the stability of the process of concrete fracture and steel plastic flow will be studied, and its dependence on the mechanical and geometrical (scale included) properties of the beam cross section will be shown. A role of primary importance, besides that of steel percentage $A_s/A$ (1), is played by the nondimensional number $f_y b^{1/2}/K_{IC}$ (analogous to the brittleness number defined in Ref. 3, which includes the mechanical properties of the materials and the sizes of the structure, i.e., $f_y$ = the yield strength of steel, $K_{IC}$ = the fracture toughness of concrete, and $b$ = the beam depth. Finally, it is surprising to verify how we can increase either the structure size or the steel area in order to obtain a real concrete fracture phenomenon. Therefore, a glimmer of light could fall on the problem of fracture testing with small specimens of aggregative materials. At this point, in fact, it seems to be confirmed that the determination of concrete fracture toughness with small specimens is meaningless, since, with small sizes, the ultimate strength collapse comes before the fracture collapse (3).

## Statically Undetermined Reaction of Reinforcement

Let us consider a reinforced concrete beam element with a rectangular cross section of thickness $t$ and depth $b$, subjected to a bending moment, $M$. Let the steel reinforcement be distant, $h$, from the external surface, while a through-thickness edge crack of depth $a \geq h$ is assumed to exist in the stretched part (Fig. 1). Therefore, the cracked concrete beam element will be subjected to the external bending moment, $M$, and to an eccentric axial force, $F$, due to the statically undetermined reaction of the reinforcement. It is well known that a bending moment, $M^*$, induces a stress-intensity factor, $K_I$, at the crack tip equal to

$$K_I = \frac{M^*}{b^{3/2} t} Y_M(\xi) \quad (1)$$

in which $\xi = a/b$ = the relative crack depth; and $Y_M$ = the function (8). For $\xi \leq 0.7$

$$Y_M(\xi) = 6 \times (1.99\xi^{1/2} - 2.47\xi^{3/2} + 12.97\xi^{5/2} - 23.17\xi^{7/2} + 24.80\xi^{9/2}) \quad (2)$$

In the same way, an axial tensile force, $F^*$, induces the stress-intensity factor (8)

$$K_I = \frac{F^*}{b^{1/2} t} Y_F(\xi) \quad (3)$$

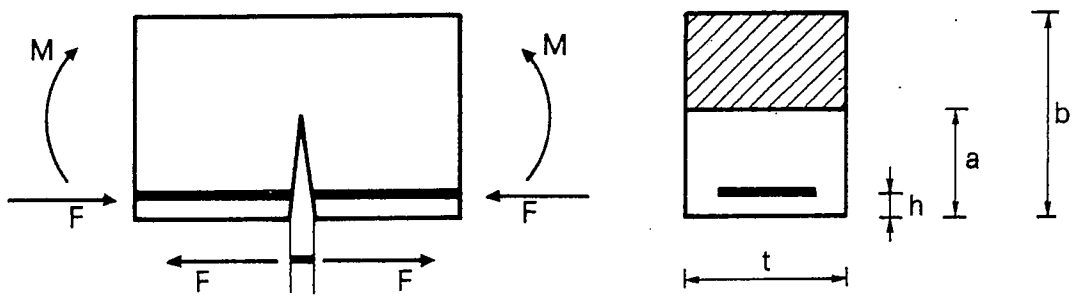


**FIG. 1.—Cracked Reinforced Beam Element**

for $\xi \leq 0.7$

$$Y_F(\xi) = 1.99\xi^{1/2} - 0.41\xi^{3/2} + 18.70\xi^{5/2} - 38.48\xi^{7/2} + 53.85\xi^{9/2} \quad (4)$$

On the other hand, the bending moment, $M^*$, causes a local rotation, $\phi$, equal (8,9) to

$$\phi = \lambda_{MM} M^* \quad (5)$$

$$\text{with} \quad \lambda_{MM} = \frac{2}{b^2 tE} \int_0^{\xi} Y_M^2(\xi) d\xi \quad (6)$$

while the axial tensile force, $F^*$, causes the rotation (8,9)

$$\phi = \lambda_{MF} F^* \quad (7)$$

$$\text{with} \quad \lambda_{MF} = \frac{2}{btE} \int_0^{\xi} Y_M(\xi)\, Y_F(\xi) d\xi \quad (8)$$

In the case of the considered statically undeterminate system, i.e., the reinforced beam element (Fig. 1), the global moment acting on the cross section will be

$$M^* = M - F\left(\frac{b}{2} - h\right) \quad (9)$$

i.e., it will be given by the external moment (opening the crack) subtracted by the reinforcement reaction moment (closing the crack). Then the axial force acting on the cross section will be

$$F^* = -F \quad (10)$$

Up to the moment when steel yields the rotation, due to the bending moment $M^*$ and to the closing force $F^*$, will be equal to zero:

$$\phi = \lambda_{MM} M^* + \lambda_{MF} F^* = 0 \quad (11)$$

Eq. 11 is the congruence condition which is able to provide the unknown $F$. Replacing Eqs. 9–11, the result is

$$\lambda_{MM}\left[M - F\left(\frac{b}{2} - h\right)\right] - \lambda_{MF} F = 0 \quad (12)$$

and finally it is possible to obtain

$$\frac{Fb}{M} = \frac{1}{\left(\frac{1}{2} - \frac{h}{b}\right) + r(\xi)} \quad (13)$$

$$\text{in which} \quad r(\xi) = \frac{\int_0^{\xi} Y_M(\xi)\, Y_F(\xi) d\xi}{\int_0^{\xi} Y_M^2(\xi) d\xi} \quad (14)$$

The statically undetermined reaction of the reinforcement, against the relative crack depth, for $h/b = 1/10$, $1/20$, is reported in Fig. 2. The

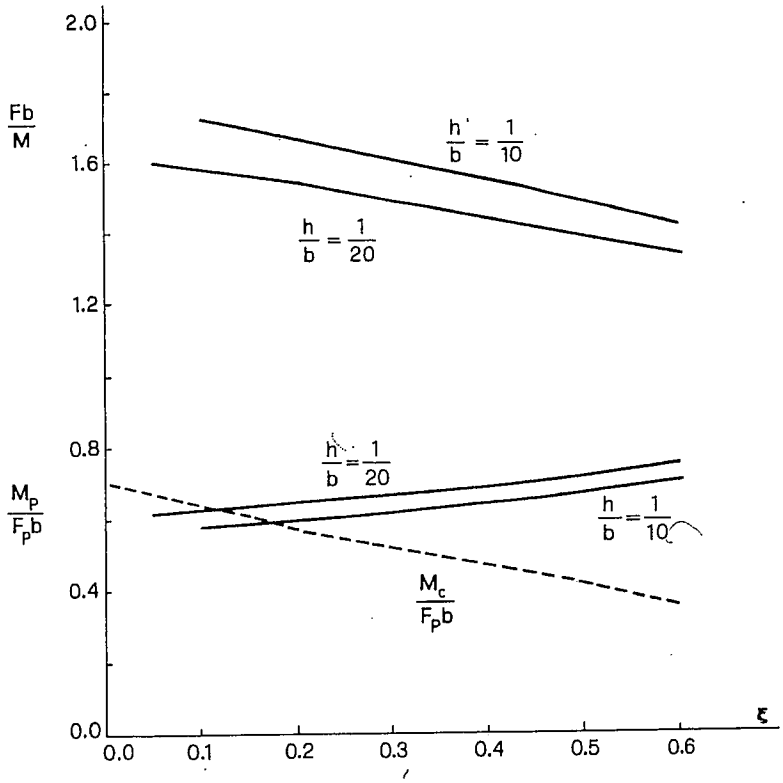


**FIG. 2.—Reaction of Reinforcement and Bending Moment of Reinforcement Plastic Flow, Due to Yielding of Steel or to Slippage of Bar**

decrease of the reaction by increasing the crack depth is not immediately understood, and, indeed, it may even surprise the reader. However, it can be explained by observing that the compliances $\lambda_{MM}$ and $\lambda_{MF}$ both increase with an increasing crack length, but $\lambda_{MF}$ increases more rapidly than $\lambda_{MM}$. Thus lower and lower axial forces, $F$, are needed to annul the rotation due to the external moment, $M$.

## Bending Moment of Reinforcement Plastic Flow Due to Yielding or Slippage

As Eq. 13 shows, the force $F$, transmitted by reinforcement, increases linearly by increasing the external moment, $M$, until the limit force, $F_P = f_y A_s$, is reached, $f_y$ being the steel yield strength and $A_s$ the steel area. Before steel yields, cracks grow in reinforced concrete only when slippage is allowed between the concrete and steel. Even if slippage is not explicitly considered in the model, it can be simulated by a fictitious yield strength, $\bar{f}_y$, of steel, lower than the real $f_y$.

In any case, a perfectly plastic behavior of the reinforcement will be considered. This means that the infinitesimal reinforcement segment, which is uncovered, i.e., included between the two crack surfaces, will flow, always transmitting the same force, $F_P$, to the cracked concrete element (Fig. 3). From Eq. 13 it is possible to obtain the moment of plastic flow for the reinforcement:

$$M_P = F_P b\left[\left(\frac{1}{2} - \frac{h}{b}\right) + r(\xi)\right] \quad \text{(15)}$$

Such a moment against the relative crack depth, for $h/b = 1/10$, $1/20$,

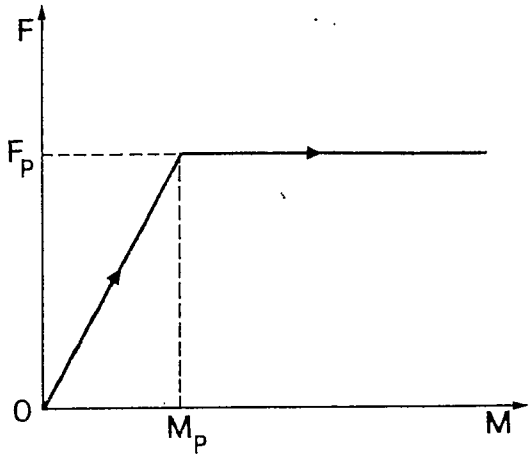


**FIG. 3.—Force Transmitted by Reinforcement Against Applied Moment**

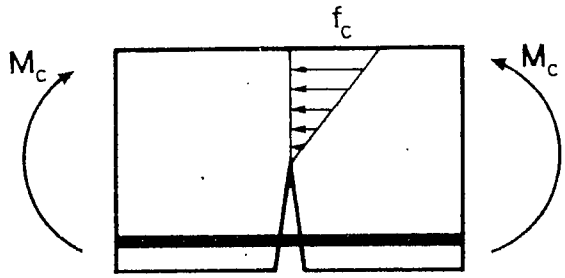


**FIG. 4.—Hypothesis of Linear Stress Variation through Ligament**

is reported in Fig. 2. According to the decrease of the reaction from increasing the crack depth, $\xi$ (Fig. 2), an increase of the moment of reinforcement plastic flow, $M_P$, occurs by increasing $\xi$.

However, it should be observed that, if concrete presents a low crushing strength, $f_c$, and steel presents a relatively high yield strength, $f_y$, the concrete crushing collapse can come before the steel plastic flow. If $M_c$ is the external moment of concrete crushing and a hypothesis of linear stress variation through the ligament holds (Fig. 4) (1), it follows that

$$\frac{M_c}{F_P b} = \frac{f_c}{f_y \dfrac{A_s}{A}} \frac{(1-\xi)\left(2+\xi-3\dfrac{h}{b}\right)}{6} \quad \text{(16)}$$

The dashed line of Fig. 2 represents the diagram of Eq. 16 for $f_c = 2.85$ ksi (19.62 MPa); $f_y = 51.26$ ksi (353.16 MPa); $A_s/A = 0.024$; and $h/b = 1/10$. It can be observed that, although values very favorable to the concrete crushing collapse have been chosen, such collapse in fact comes before the steel plastic flow only for sufficiently high values of the crack depth ($\xi \geq 0.175$).

## Rigid-Hardening Behavior of Cracked Beam Section

This section describes the mechanical behavior of the cracked reinforced concrete beam section, once the bending moment, $M_P$, of steel plastic flow has been exceeded. For $M \leq M_P$ we have $\phi = 0$, while for $M > M_P$

$$\phi = \lambda_{MM}\left[M - F_P\left(\frac{b}{2} - h\right)\right] - \lambda_{MF} F_P \quad \text{(17)}$$

The $M$-$\phi$ diagram is represented in Fig. 5. This diagram expresses the equivalence of the beam section with a rigid-linear hardening spring. It is interesting to observe that the hardening line is parallel to the $M$-$\phi$ diagram relating to the same cracked beam section without reinforcement (broken line).

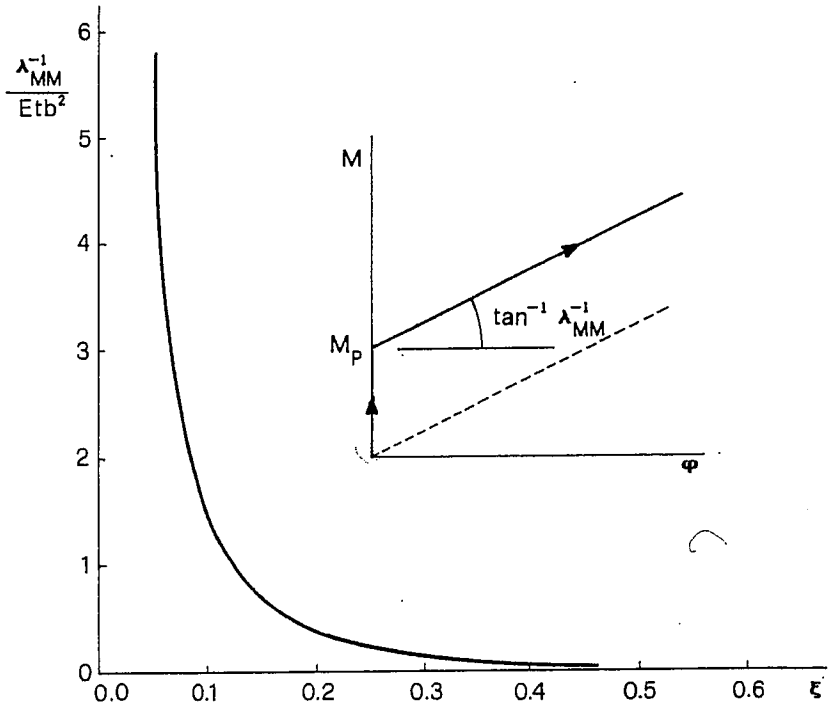


**FIG. 5.—Hardening Coefficient Against Relative Crack Depth**

The hardening coefficient $\lambda^{-1}_{MM}$ against the relative crack depth $\xi$ is reported again in Fig. 5. By increasing the crack depth, $\xi$, the hardening line becomes more and more inclined, until giving rigid-perfectly-plastic behavior. On the other hand, for $\xi \rightarrow 0$, the hardening line becomes nearly vertical, until giving a rigid behavior of the beam section simulating spring.

Therefore, it is possible to conclude that, by increasing $\xi$, the moment of steel plastic flow increases (Fig. 2), while the slope of the hardening line decreases (Fig. 5). Some $M$-$\alpha$ diagrams, for $h/b = 1/20$, are reported in Fig. 6 with $\xi$ varying between 0.05 and 0.50. The moment of steel plastic flow increases very little by increasing $\xi$; on the other hand, the slope of the hardening line decreases sharply.

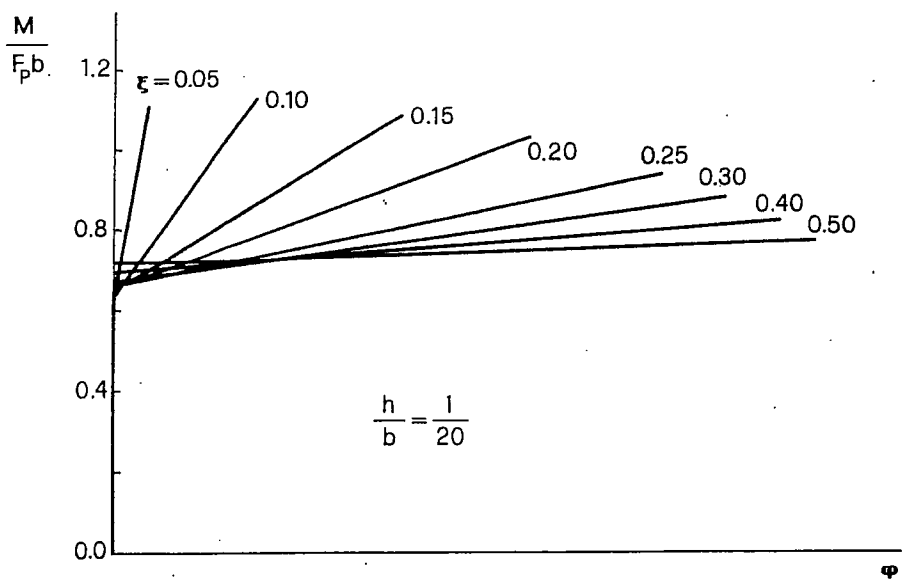


**FIG. 6.—Moment-Rotation Diagrams for Different Crack Depths**

## Bending Moment of Concrete Fracture

In this section, crack growth in concrete will be examined. It is consequent to the steel plastic flow, i.e., it occurs for a bending moment, $M_F \geq M_P$.

After the steel plastic flow, the stress-intensity factor acting at the crack tip will be equal to the algebraical addition of Eqs. 1 and 3, and the actual loadings will be

$$M^* = M - F_P\left(\frac{b}{2} - h\right) \quad (18)$$

$$F^* = -F_P \quad (19)$$

$$\text{Thus} \quad K_I = \frac{1}{b^{3/2}t} Y_M(\xi)\left[M - F_P\left(\frac{b}{2} - h\right)\right] - \frac{F_P}{b^{1/2}t} Y_F(\xi) \quad (20)$$

Presuming that Eq. 20 is equal to the concrete fracture toughness, $K_{IC}$, it is possible to obtain the fracture moment $M_F$:

$$M_F = \frac{K_{IC} b^{3/2} t}{Y_M(\xi)} + \frac{F_P b}{Y_M(\xi)}\left[Y_F(\xi) + Y_M(\xi)\left(\frac{1}{2} - \frac{h}{b}\right)\right] \quad (21)$$

In nondimensional form

$$\frac{M_F}{K_{IC} b^{3/2} t} = \frac{1}{Y_M(\xi)} + N_P\left[\frac{Y_F(\xi)}{Y_M(\xi)} + \frac{1}{2} - \frac{h}{b}\right]$$

$$\text{in which} \quad N_P = \frac{f_y b^{1/2}}{K_{IC}} \cdot \frac{A_s}{A} \quad (22)$$

The concrete fracture moment, $M_F$, against the relative crack depth, $\xi$, is shown in Fig. 7, varying the nondimensional number $N_P$ ($h/b = 1/20$).

For $N_P$ values close to zero, i.e., for low reinforced beams or for very small cross sections, the fracture moment decreases while the crack extends, and a typical phenomenon of unstable fracture occurs.

For higher $N_P$ values, a stable branch follows the unstable one of the curve, which describes the crack extension against the applied load. Immediately, for $N_P = 1$, the minimum of the curve is evident and takes place for $\xi \simeq 0.35$. For higher $N_P$ values, the $\xi$ value for which the minimum occurs is lower, while the stable branch becomes steeper and steeper. For $N_P \gtrsim 8.5$, the unstable branch disappears and only the stable branch remains.

Analogous behavior has been underlined in the case of a cracked masonry wall, subjected to an eccentric axial compression force (7). In that case, however, the unstable branch and the consequent stable one appear steeper and the existence of the minimum is then more evident.

The locus minimorum is represented by a dashed line in Fig. 7. This line divides the quadrant of the diagram into two zones: the upper zone is where the fracturing process is stable, while the lower one is where the process is unstable. It is therefore possible to assert that the fracturing process in reinforced concrete becomes stable only when the beam

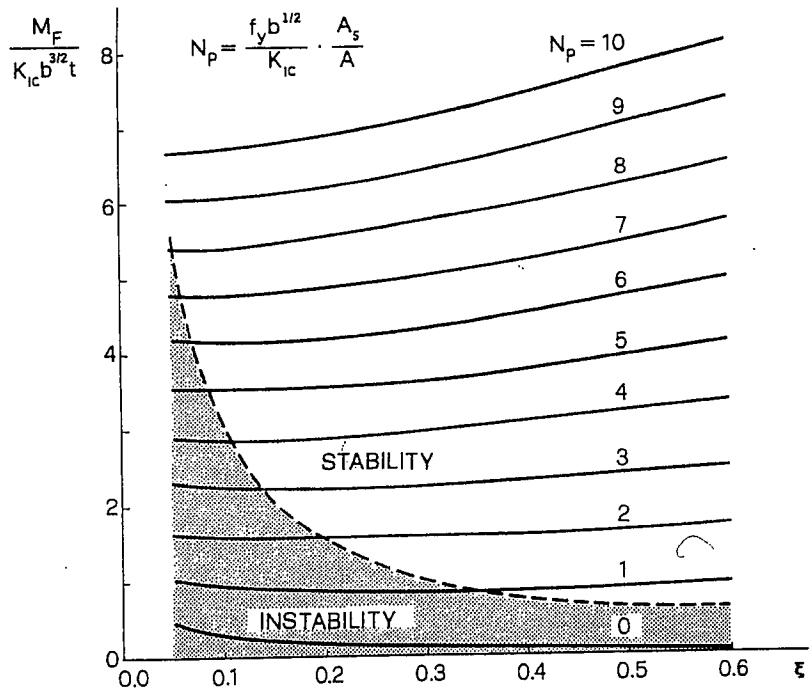


**FIG. 7.—Bending Moment of Crack Propagation Against Relative Crack Depth ($h/b$ = 1/20)**

is sufficiently reinforced or the cross section is sufficiently large, and when the crack is sufficiently deep.

If the curve $N_P$ = constant were perfectly horizontal, a condition of indifferent equilibrium would occur. In fact, none of the curves shows such a regularity. However, it is important to observe that the curve relating to $N_P = 1$, which could represent the fracturing phenomenon for very common reinforced concrete beams, is only slightly deflected downwards: the minimum is only about 15% lower than the value of the function for $\xi = h/b = 0.05$.

For $h/b = 1/10$, curves very similar to those of Fig. 7 are obtained. Only two slight differences are present: (1) The curves go down, i.e., fracture collapse occurs for lower moments, since the reinforcement, being internal, resists to a lesser extent than in the preceding case; and (2) the dashed line goes up, i.e., the stable zone of the diagram shrinks.

Finally, it may be interesting to compute the nondimensional number, $N_P$, for three different reinforced concrete beams. As a first example, let us consider the following set of values: $f_y$ = 34.17 ksi (235.44 MPa); $K_{IC}$ = 715.2 psi $\sqrt{\text{in.}}$ (0.78 MN m$^{-3/2}$); $b$ = 11.81 in. (30 cm); $A_s/A$ = 0.01; from which one obtains: $N_P = 1.64$.

Thus, it is possible to verify in Fig. 7 that, for this very common reinforced concrete beam, the fracturing process is very close to a condition of indifferent equilibrium. Let us now examine a low reinforced beam with small cross section: $f_y$ = 34.17 ksi (235.44 MPa); $K_{IC}$ = 894 psi $\sqrt{\text{in.}}$ (0.98 MN m$^{-3/2}$); $b$ = 7.87 in. (20 cm); $A_s/A$ = 0.0024; from which it follows: $N_P = 0.26$. In this beam the fracturing process occurs in an unstable manner (Fig. 7).

As a third and last case, let us examine a high reinforced beam with large cross section: $f_y$ = 51.26 ksi (353.16 MPa); $K_{IC}$ = 447 psi $\sqrt{\text{in.}}$ (0.49 MN m$^{-3/2}$); $b$ = 59.05 in. (150 cm); $A_s/A$ = 0.0240; from which results

$N_P = 21.16$. In this beam the fracturing process occurs in a stable manner (Fig. 7).

## Stability of Process of Concrete Fracture and Steel Plastic Flow

In this section, fracture stability will be studied using energy considerations. The stress-intensity factor acting on the crack is

$$K_I = \frac{1}{b^{3/2}t} Y_M(\xi)\left[M - F\left(\frac{b}{2} - h\right)\right] - \frac{1}{b^{1/2}t} Y_F(\xi) F, \quad \text{for} \quad M \le M_P \quad \ldots (23)$$

$$K_I = \frac{1}{b^{3/2}t} Y_M(\xi)\left[M - F_P\left(\frac{b}{2} - h\right)\right] - \frac{1}{b^{1/2}t} Y_F(\xi) F_P, \quad \text{for} \quad M > M_P \quad (24)$$

Replacing Eq. 13 in Eq. 23 gives

$$K_I = \frac{1}{b^{3/2}t} Y_M(\xi)\left[M - \frac{M}{b}\frac{1}{\left(\frac{1}{2} - \frac{h}{b}\right) + r(\xi)}\left(\frac{b}{2} - h\right)\right]$$

$$- \frac{1}{b^{1/2}t} Y_F(\xi) \frac{M}{b} \frac{1}{\left(\frac{1}{2} - \frac{h}{b}\right) + r(\xi)}, \quad \text{for} \quad M \le M_P \quad \ldots\ldots\ldots\ldots\ldots\ldots (25)$$

Eqs. 25 and 24 in nondimensional form appear as follows:

$$\frac{K_I b^{1/2} t}{F_P} = Y_M(\xi) \frac{M}{F_P b}\left[1 - \frac{1}{1 + \frac{r(\xi)}{\left(\frac{1}{2} - \frac{h}{b}\right)}}\right]$$

$$- \frac{M}{F_P b} Y_F(\xi) \frac{1}{\left(\frac{1}{2} - \frac{h}{b}\right) + r(\xi)} \quad \text{for} \quad M \le M_P \quad \ldots\ldots\ldots\ldots\ldots\ldots (26)$$

$$\frac{K_I b^{1/2} t}{F_P} = Y_M(\xi)\left[\frac{M}{F_P b} - \left(\frac{1}{2} - \frac{h}{b}\right)\right] - Y_F(\xi), \quad \text{for} \quad M > M_P \quad \ldots\ldots\ldots (27)$$

The stress-intensity factor, $K_I$, against the crack depth, $\xi$, is reported in Fig. 8, varying the loading parameter $M/F_P b$ ($h/b = 1/20$). For $M/F_P b$ values lower than about 0.7, the stress-intensity factor is very low for every considered depth, $h/b \le \xi \le 0.6$. As the curve $M/F_P b = 0.7$ clearly shows, the $K_I$ value is positive for small depths, $\xi$, while it becomes negative for larger depths. This means that, for $0 \le M/F_P b \le 0.8$, and sufficiently deep cracks, the assumed model predicts the closing of the crack as well as the non-plastic state of steel. The plastic limit, as Fig. 2 suggests, is very near the curve, $M/F_P b = 0.7$, reported in Fig. 8. More precisely, it is included between the two curves $M/F_P b = 0.60$ and $M/F_P b = 0.75$.

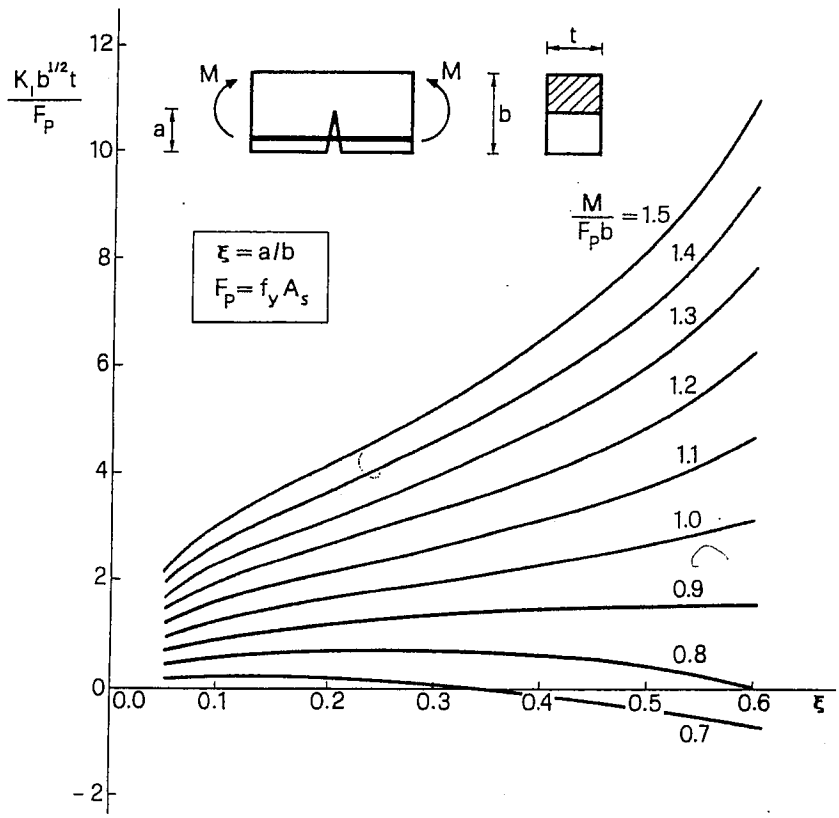


**FIG. 8.—Stress-Intensity Factor Against Relative Crack Depth, Varying Applied Moment ($h/b$ = 1/20)**

For $M/F_P b > 0.8$, the $K_I$ factor is positive for every investigated depth, $\xi$. For $M/F_P b \lesssim 0.9$, the function $K_I(\xi)$ presents a positive maximum. This means that, for sufficiently low bending moments and sufficiently deep cracks, the fracturing process is stable. In fact, from an energy point of view, we can assert that the generalized crack extension force, $\mathcal{G}_I = K_I^2/E$, has the same course of $K_I$, for $M/F_P b > 0.8$. Thus, for $0.8 \lesssim M/F_P b \lesssim 0.9$ and for sufficiently high, $\xi$

$$\frac{\partial \mathcal{G}_I}{\partial \xi} = -\frac{\partial^2 V}{\partial \xi^2} < 0 \qquad (28)$$

in which $V$ = the total potential energy of the concrete-steel system. In other words, for those particular values of bending moment and crack depth, the total potential energy, $V$, can present, as a stationary value ($K_I = K_{IC}$), only a minimum and therefore a stable equilibrium condition.

## Fracture Sensitivity Increase due to Reinforcement

Up to now, no indication of how much the fracture moment, $M_F$, is higher than the plastic flow moment, $M_P$, has been given. From Eqs. 15 and 21, it follows that

$$\frac{M_P}{M_F} = \frac{\left[\frac{1}{2} - \frac{h}{b} + r(\xi)\right] Y_M(\xi)}{\frac{1}{N_P} + Y_F(\xi) + Y_M(\xi)\left(\frac{1}{2} - \frac{h}{b}\right)} \qquad (29)$$

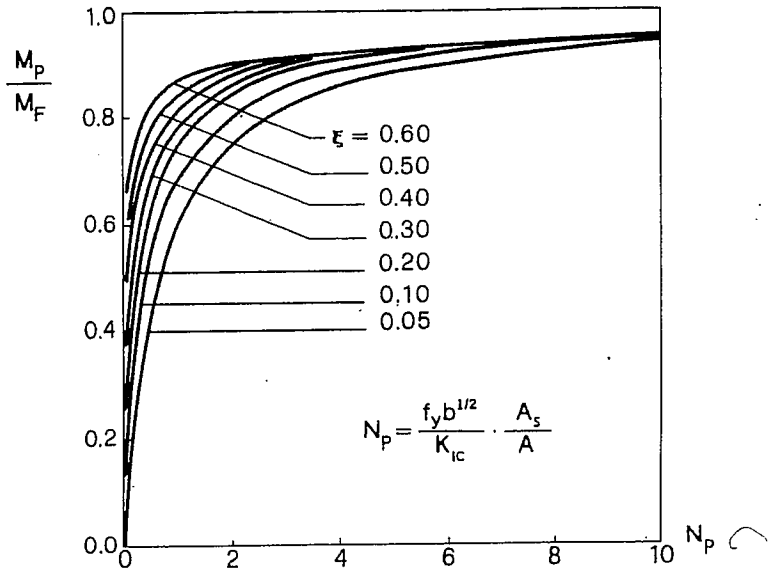


**FIG. 9.—Ratio between Moment of Steel Plastic Flow and Moment of Concrete Fracture, Against Nondimensional Number $N_P$, Varying Relative Crack Depth, ξ ($h/b$ = 1/20)**

In Fig. 9, the ratio $M_P/M_F$ against the nondimensional number, $N_P$, is represented, varying the crack depth, ξ ($h/b$ = 1/20). From this diagram we deduce that the higher the number, $N_P$, and the deeper the crack, the closer the crack propagation is to steel plastic flow. This means that the fracture collapse can be obtained immediately after the plastic one by varying two parameters: (1) The beam size, $b$; and (2) the steel percentage, $A_s/A$.

Of the five potential collapses mentioned in the Introduction, only three have been explicitly considered up to now. Eq. 16 shows that the concrete crushing collapse tends to precede the others for high steel percentages, $A_s/A$. Once such a collapse has been avoided, the other four are to be considered. The steel flow due to plastic deformation or to slippage is certainly the first to be reached, while the ultimate strength collapse and the crack propagation in concrete follow with a priority which is difficult to estimate.

In the field of fracture toughness testing, it is in the experimenter's interest that a real fracture phenomenon occurs in concrete, i.e., that the crack extension is due to the fracture toughness overcoming rather than to the ultimate strength overcoming. In a preceding paper (3) the writer has explained that this goal can be reached, with nonreinforced specimens, simply by considering sufficiently large specimen sizes. In the case of reinforced fracture specimens and in the most unfavorable hypothesis, the ultimate strength collapse could precede the fracture collapse; on the other hand, it should follow the steel plastic flow. For example, in the case $h/b = 0.05$, $\xi = 0.10$, $N_P = 10$, the result is $M_P/M_F \simeq 0.95$ (Fig. 9), and then the ultimate strength moment, $M_u$, would be included in a very narrow interval, $0.95\ M_F \leq M_u \leq M_F$, which immediately precedes the fracture moment, $M_F$.

Therefore, the possibility of increasing the concrete fracture sensitivity, simply by reinforcing the fracture specimen, stands out. According to the previous analysis, this operation appears to be exactly the same

as that of increasing the specimen sizes. In both cases, in fact, the same effect of increasing the system capacity, as for an elastic energy container, is attained.

Thus, according to the utilized fracture model, one can conclude that the collapses for steel plastic flow, for concrete ultimate strength, and for crack propagation, tend to coincide, by increasing $N_P$, i.e., by increasing the specimen sizes or the steel percentage.

A serious problem lies in the fact that the experimenter does not know a priori the number, $N_P$, of the test which he is going to perform, since he does not know $K_{IC}$. Thus, he does not know the ratios between $M_P$, $M_u$, $M_F$. This handicap could probably be eliminated through iterative experimental techniques of progressive approach to the real $K_{IC}$ value. However, a very slight variation of the ratio $M_P/M_F$ occurs for $\xi \gtrsim 0.20$ and $N_P \gtrsim 2$ (Fig. 9).

## Synthesis and Concluding Remarks

In Fig. 10 the moment-rotation diagrams, $M(\phi)$, are reported for $h/b = 1/20$, $\xi = 0.1$, and for five different values of number $N_P$: 0.0, 0.1, 0.3, 0.7, and 3.0. Once the cross section sizes and the mechanical properties of the material have been defined, they represent five different steel areas.

Rigid behavior ($0 \leq M \leq M_P$) is followed by linear hardening behavior ($M_P < M \leq M_F$). The latter stops when crack propagation occurs. If the fracture phenomenon is unstable, function $M(\phi)$ presents a discontinuity and drops from value $M_F$ to value $F_P b$ with a negative jump [Figs. 10(*a*)–(*d*)]. In fact, in this case a complete and instantaneous disconnection of the concrete cross section occurs. While the rotation, $\phi$, is constant, the new moment, $F_P b$, can be estimated according to the scheme of Fig. 11, where each beam segment is subjected to the traction, $F_P$, of the reinforcement and to the contact compression, $F_P$, i.e., altogether, to the moment $F_P(b - h) \simeq F_P b$. Then, increasing the rotation, $\phi$, and ignoring any phenomenon of instability, the bending moment decreases with a nonlinear law (Fig. 11):

$$M = F_P b \cos \frac{\phi}{2} \qquad (30)$$

On the other hand, if the fracture phenomenon is stable, function $M(\phi)$ does not present any discontinuity and describes hardening behavior [Fig. 10(*e*)] analogous to that of Fig. 6.

In Fig. 10(*a*), the case $N_P = 0$ is considered, i.e., the beam without reinforcement. The plastic flow moment, $M_P$, is naturally equal to zero, as well as the moment $F_P b$, which occurs immediately after the complete disconnection of concrete.

In Fig. 10(*b*), the case $N_P = 0.1$ is described, i.e., a low reinforced beam. With Fig. 2, it is possible to obtain the ratio $M_P/F_P b$, and with Fig. 9, the ratio $M_P/M_F$. The slope of the hardening line does not vary with respect to the preceding case, since it depends only on the crack length, besides the concrete elastic modulus and the cross section sizes (Fig. 5).

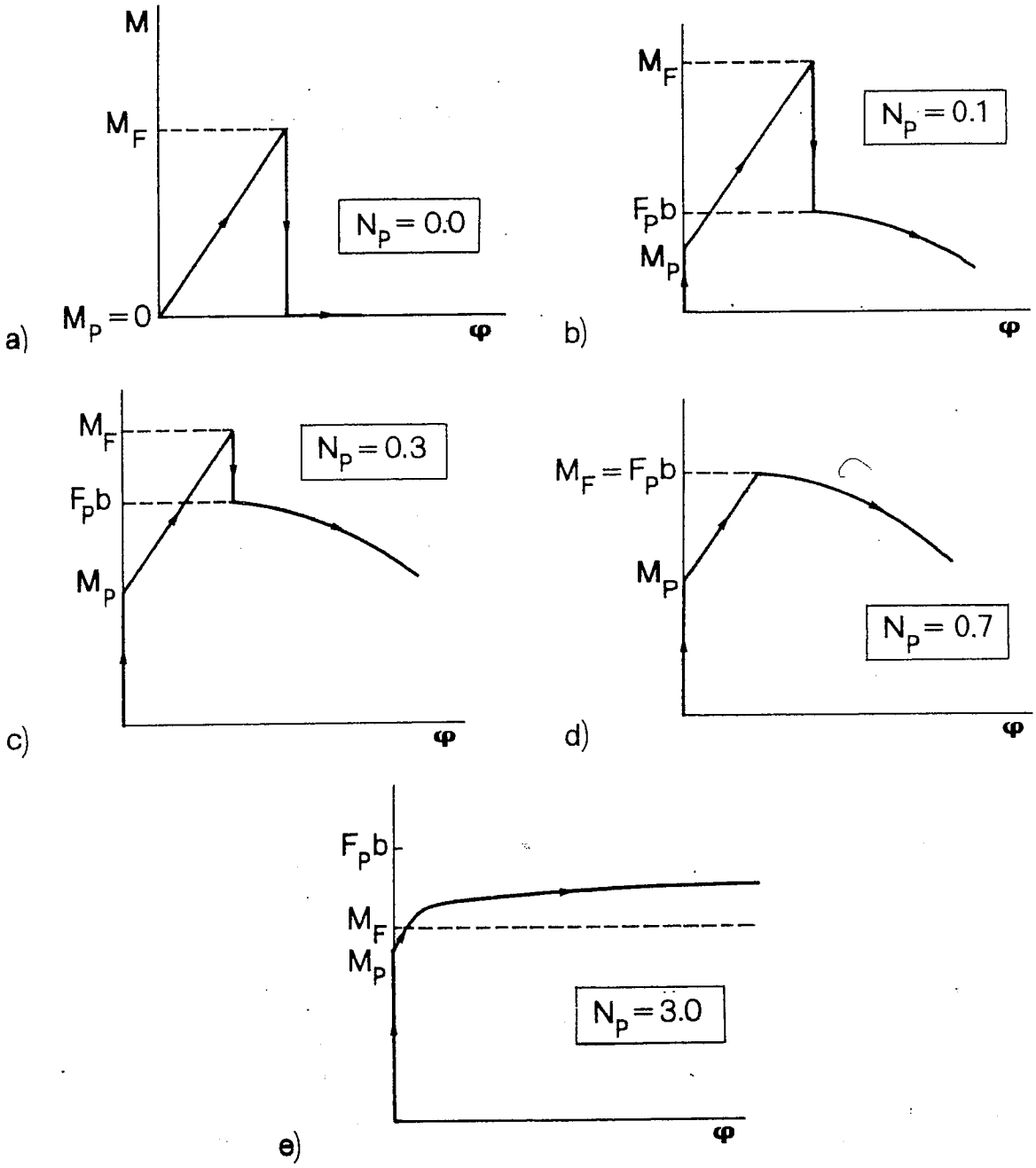


**FIG. 10.—Mechanical Behavior of Cracked Reinforced Beam Section, for Different Nondimensional Numbers, $N_P$ ($h/b$ = 0.05; $\xi$ = 0.10)**

In Fig. 10(*c*) the case $N_P = 0.3$ is considered, which is analogous to the previous one, except for the fact that the ratio $M_P/M_F$ is higher. On the other hand, the ratio $M_P/F_P b$, which is independent of $N_P$ (Fig. 2), remains unchanged. In Fig. 10(*d*) the case $N_P = 0.7$ is reported. For this value it is $M_F = F_P b$, and then the discontinuity vanishes.

Finally, in Fig. 10(*e*) the case $N_P = 3$ is described. In this case the fracture moment, $M_F$, is only slightly higher than the plastic moment, $M_P$, and the moment $F_P b$ would be obtainable only with a positive jump of the function. On the other hand, from Fig. 7 it is known that the fracturing process, for $N_P = 3$ and $\xi \geq 0.14$, is stable and, thus, a complete and instantaneous disconnection of concrete cannot occur (Fig. 11).

It is observed that for $N_P \leq 0.7$, $F_P b \leq M_F$, and then a discontinuity appears in the diagram, $M(\phi)$ [Figs. 10(*a*)–(*d*)], so for $N_P \leq 0.7$, the curves of Fig. 7 lie completely in the unstable zone. Therefore, it is possible to

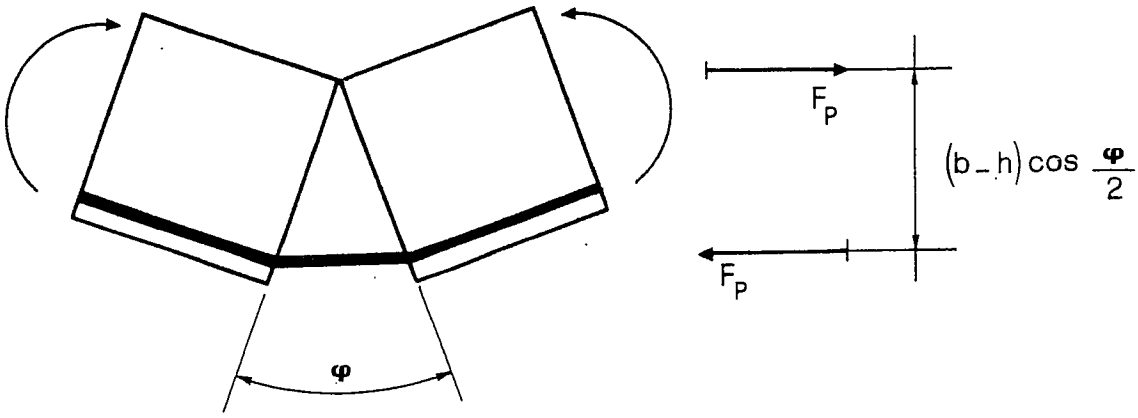


**FIG. 11.—Statical Scheme after Complete Disconnection of Concrete**

conclude that, by increasing the steel percentage, $A_s/A$, or, in the same way, by increasing the beam size, $b$, the concrete fracturing process becomes stable.

## Acknowledgments

The writer gratefully acknowledges the research support of the Italian National Research Council (C.N.R.).

## Appendix I.—References

1. Avram, C., Filimon, I., Deutsch, I., and Clipii, T., "Crack Control and Crack Widths in Low Reinforced Concrete Members," Corso di Perfezionamento per le Costruzioni in Cemento Armato *Fratelli Pesenti*, Politecnico di Milano, Milan, Italy, 1979, pp. 259–319.
2. Carpinteri, A., "Size Effect in Fracture Toughness Testing: A Dimensional Analysis Approach," *Analytical and Experimental Fracture Mechanics*, G. C. Sih and M. Mirabile, eds., Sijthoff & Noordhoff, 1981, pp. 785–797.
3. Carpinteri, A., "Notch Sensitivity in Fracture Testing of Aggregative Materials," *Engineering Fracture Mechanics*, Vol. 16, No. 4, 1982, pp. 467–481.
4. Carpinteri, A., "Experimental Determination of Fracture Toughness Parameters $K_{IC}$ and $J_{IC}$ for Aggregative Materials," *Advances in Fracture Research*, D. Francois, ed., Pergamon Press, New York, N.Y., 1981, pp. 1491–1498.
5. Carpinteri, A., "Static and Energetic Fracture Parameters for Rocks and Concretes," *Materials & Structures*, Vol. 14, No. 81, 1981, pp. 151–162.
6. Carpinteri, A., Di Tommaso, A., and Viola, E., "Fatigue Evolution of Multicracked Frame-Structures," *Analytical and Experimental Fracture Mechanics*, G. C. Sih and M. Mirabile, eds., Sijthoff & Noordhoff, 1981, pp. 417–430.
7. Carpinteri, A., Di Tommaso, A., and Viola, E., "On the Limit Bearing Capacity of Cracked Masonry Walls," *Proceedings of the 5th Congress of the Italian Association of Theoretical and Applied Mechanics*, Palermo, Italy, 1980.
8. Okamura, H., Watanabe, K., and Takano, T., "Applications of the Compliance Concept in Fracture Mechanics," *ASTM STP 536*, 1973, pp. 423–438.
9. Okamura, H., Watanabe, K., and Takano, T., "Deformation and Strength of Cracked Member Under Bending Moment and Axial Force," *Engineering Fracture Mechanics*, Vol. 7, 1975, pp. 531–539.
10. "Raccomandazioni CEB/FIP per le Strutture in Cemento Armato," *Edizione Italiana A.I.T.E.C.*

## Appendix II.—Notation

*The following symbols are used in this paper:*

$A$ = total area of cross section;
$A_s$ = steel area;
$a$ = crack depth;
$b$ = depth of beam;
$E$ = Young's modulus of concrete;
$F$ = statically undetermined reaction of reinforcement;
$F_P = f_y A_s$ = force of plastic flow collapse for reinforcement;
$f_c$ = compressive strength of concrete;
$f_u$ = tensile strength of concrete;
$f_y$ = yield strength of steel;
$h$ = distance of reinforcement from external surface;
$K_I$ = stress-intensity factor;
$K_{IC}$ = fracture toughness of concrete;
$M$ = bending moment;
$M_F$ = bending moment of crack propagation;
$M_P$ = bending moment of steel plastic flow;
$N_P$ = $(f_y b^{1/2}/K_{IC})(A_s/A)$ = nondimensional number;
$r$ = ratio defined in Eq. 14;
$Y_M, Y_F$ = functions defined in Eqs. 2 and 4;
$t$ = thickness of beam;
$\xi$ = $a/b$ = relative crack depth;
$\lambda_{MM}, \lambda_{MF}$ = rotational compliances due to bending moment and axial force; and
$\phi$ = local rotation at cracked cross section.